Electronic Supplementary Material (ESI) for RSC Advances.
This journal is © The Royal Society of Chemistry 2021

Supplementary Information

Enhanced negative magnetoresistance near the charge neutral point in Cr doped topological insulator

Qixun Guo[1], Yu Wu[1,2], Dongwei Wang[3], Gang Han[4], Xuemin Wang[4], Libo Fu[5], Lihua Wang[5], Wei He[6], Tao Zhu[6], Zhendong Zhu[7], Tao Liu[8], Guanghua Yu[1], Jiao Teng[1*]

[1]Department of Material Physics and Chemistry, University of Science and Technology Beijing, Beijing 100083, P. R. China

[2]Beijing Tongfang Huachuang Technology Co., Ltd., Beijing 100089, P. R. China

[3]CAS Key Laboratory of Standardization and Measurement for Nanotechnology, National Center for Nanoscience and Technology, Beijing 100190, P. R. China

[4]Collaborative Innovation Center of Advanced Steel Technology, University of Science and Technology Beijing, Beijing 100083, P. R. China

[5]Institute of Microstructure and Property of Advanced Materials, Beijing Key Lab of Microstructure and Property of Advanced Materials, Beijing University of Technology, Beijing 100124, P. R. China

[6]Beijing National Laboratory for Condensed Matter Physics and Institute of Physics, Chinese Academy of Sciences, Beijing 100190, P. R. China

[7]National Institute of Metrology, Beijing 100029, P. R. China

[8]National Engineering Research Center of Electromagnetic Radiation Control Materials, University of Electronic Science and Technology of China, Chengdu 610054, P. R. China

Figure S1. (a) Scheme of co-sputtering process and crystal structure of CBST. (b) High-resolution TEM (HRTEM) image of a CBST thin film. (c, d) HRTEM image of the red square in (b) and corresponding FFT pattern.

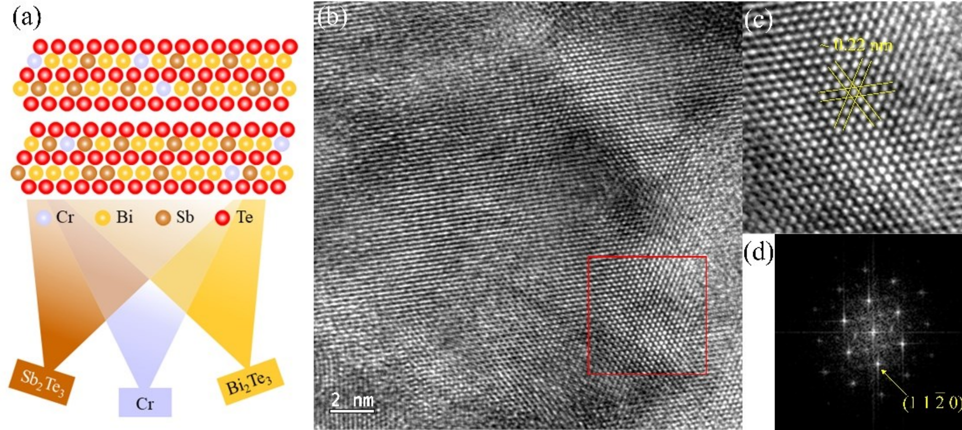

We use magnetron co-sputtering to fabricate CBST thin films (Fig. S1(a)). A chemical etch by hydrofluoric acid is performed to remove the SiO_2 under the CBST sample, leaving the large area CBST thin films. Then we transferred the free-standing CBST thin film onto a holey carbon support film. High-resolution TEM (HRTEM) image of the CBST2 thin film (Fig. S1(c)) and fast Fourier transformation (FFT) pattern (Fig. S1(d)) show the hexagonal lattice with a lattice spacing of 2.2 Å, consistent with the spacing of the (1 1 -2 0) planes of layered Bi_2Se_3[1,2].

Figure S2. The MR curves at different temperatures of CBST1(a), CBST2(b) and CBST3(c).

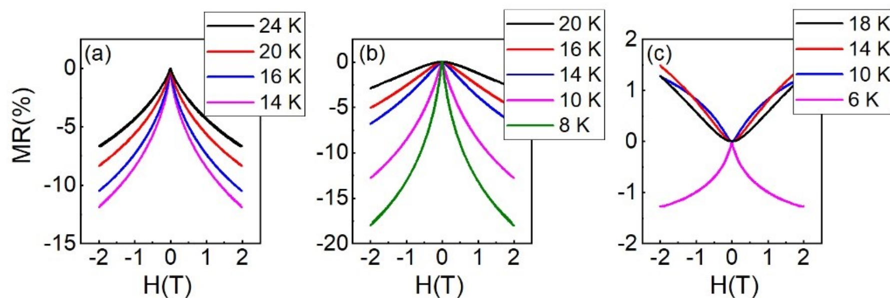

For CBST1 and CBST2, the MR is always negative below 20 K. The negative MR is similar to that commonly observed in dilute magnetic semiconductors, in which the ferromagnetism is originated from the hole-mediated coupling between magnetic

dopants based on the RKKY interaction[3-6]. In the RKKY mechanism, the Curie temperature T_c is proportional to $p^{1/3}$, where p is the hole density[7]. Therefore, the p-type CBST1 sample has the highest T_c (Fig. 3(e)), which can be attributed to enhancing the RKKY-like ferromagnetism due to the highest hole density in this sample. Given the fact that the hole-mediated RKKY interaction is completely suppressed in a system with only electron carriers, the ferromagnetism in CBST3 is dominant by the carrier-independent van Vleck mechanism. For CBST3, the evolution of MR with decreasing temperature is complex. At $T > T_c$ (11 K), there is no long-range ferromagnetic order, and a positive MR is observed (Fig. S2(c)), which is common in pristine topological insulator due to the WAL of surface states. At T =10 K (near the T_c), the MR is still positive, and the curve in the small field is sharper than that of T=14 and 18 K, which means stronger WAL at lower temperatures. However, at the large magnetic field, the MR curve increases more slowly than the 14 and 18 K curves. The MR behavior at T =10 K can be described as the competition of topology-induced WAL and magnetism-induced negative MR, and the WAL is stronger than magnetism-induced negative MR. For T= 6 K < T_c, the ferromagnetism is strong enough to cause the negative MR. Therefore, the complex MR behavior reflects the competition between topology-induced WAL and magnetism-induced negative MR[8].

Figure S3. Arrott plots at various temperatures near T_c for CBST1(a), CBST2(b) and CBST3(c). The T_cs of CBST1, CBST2 and CBST3 are 21, 11 and 12 K, respectively.

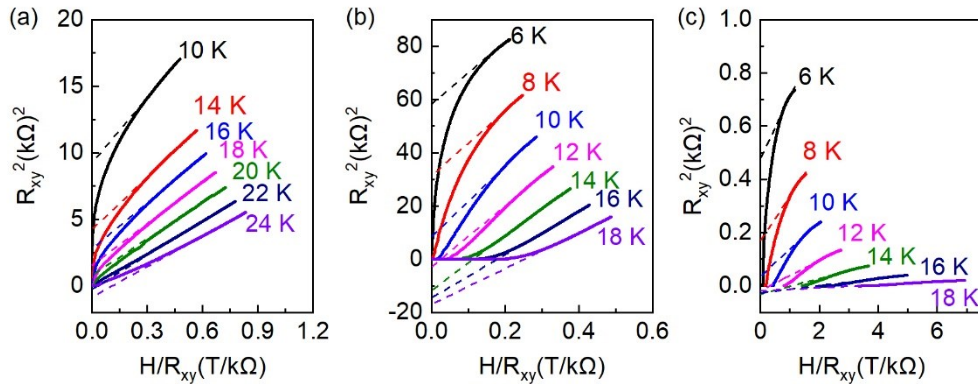

Figure S4. X-ray diffraction (XRD) patterns for magnetically doped CBST1, CBST2, CBST3 (a) and pristine BST (b) samples.

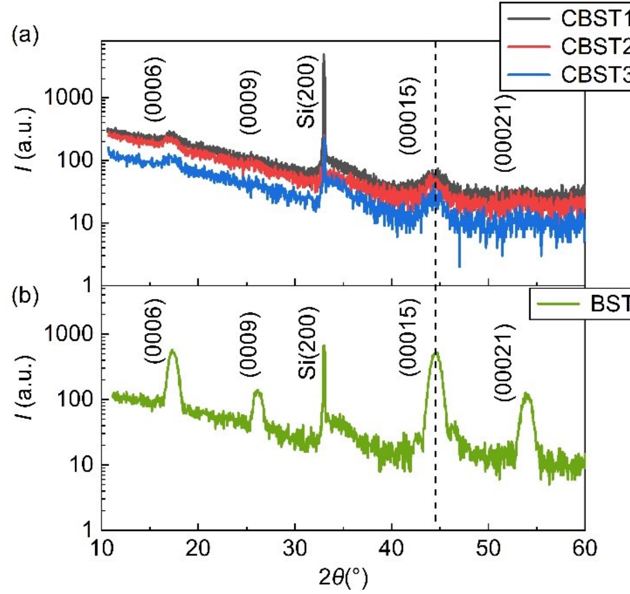

In fig. S4, the CBST and BST samples only have (0 0 0 3n) peaks, indicating that the samples have preferred orientation of c-axis, which is consistent with the results in ref. 9. We have noticed that the XRD peaks of our Cr doped samples are much weaker than the pristine BST sample, revealing the presence of a strong disorder due to the Cr doping. There is no shift of the XRD peak positions among CBST1, CBST2, and CBST3, revealing that the lattice constants of the c-axis for three samples are very similar. Besides, there is no obvious shift of (0 0 0 15) peaks of the Cr doped samples and pristine BST, indicating the Cr doping in our sample does not change the c lattice parameter. Because the ionic radius of Cr is smaller than that of Bi, the unchanged c lattice parameter indicates that Cr not only substitutes Bi atoms but also locates in the Van der Waals gaps between quintuple layers.

Table 1 The dielectric constants (ε_r) and electric-field-induced areal charge density (Δn) using the following dielectrics as gate materials.

	SiO_2	Al_2O_3	$SrTiO_3$	ionic liquid
Max voltage(V)	120	11	210	2
ε_r	3.9	9	20000	10
Thickness(nm)	300	15	200000	1

The electric-field-induced areal charge density (Δn) can be calculated using the equation $\Delta n = \varepsilon_0\varepsilon_r V_g/et$, where ε_0 and ε_r are the permittivities of vacuum and dielectrics, respectively; e is the electron charge; V_g is the electric voltage applied to the dielectrics; t is the thickness of dielectrics. Using ε_{SiO2} =3.9, ε_{Al2O3} =9, t_{SiO2} =300 nm, t_{Al2O3} =15 nm, $V_{g,SiO2}$=120 V and $V_{g,Al2O3}$=11 V, $\Delta n_{Al2O3}/\Delta n_{SiO2}$ is estimated to be 4, that is, Al_2O_3 as a dielectric is 4 times the tunability of the carrier density of SiO_2. Besides, both of $SrTiO_3$ and ionic liquid, also commonly used dielectrics, have much larger tunability of the carrier density than SiO_2.

In the previous work[10], for the same sample, three regions (hole-doped, electron-hole puddles, and electron-doped regions) can be observed by tuning the gate voltage. However, limited to the relatively weak tunability of Si/SiO_2 substrate, it is hard to observe more than one region for one sample. Therefore, in this work, changing the Bi/Sb ratio is a coarse tune of the Fermi level and carrier density. To realize accurate and continuous tuning of the Fermi level and carrier density, electric-field gating is also employed.

References

[1]D. Kong, W. Dang, J. J. Cha, H. Li, S. Meister, H. Peng, Z. Liu, and Y. Cui, Nano Lett. **10**, 2245 (2010).

[2]L. Bao, L. He, N. Meyer, X. Kou, P. Zhang, Z. G. Chen, A. V. Fedorov, J. Zou, T. M. Riedemann, T. A. Lograsso, K. L. Wang, G. Tuttle, and F. Xiu, Sci. Rep. **2**, 726 (2012).

[3]Tomasz Dietl and Hideo Ohno, Rev. Mod. Phys. **86**, 187 (2014).

[4]Yu Wu, Qixun Guo, Qi Zheng, Xiulan Xu, Tao Liu, Yang Liu, Yu Yan, Dongwei Wang, Shibing Long, Lijin Wang, Shanwu Yang, Jiao Teng, Shixuan Du, and Guanghua Yu, The Journal of Physical Chemistry C **123**, 3823 (2019).

[5]Wenbo Wang, Yunbo Ou, Chang Liu, Yayu Wang, Ke He, Qi-Kun Xue, and Weida Wu, Nat. Phys. **14**, 791 (2018).

[6]X. F. Kou, M. R. Lang, Y. B. Fan, Y. Jiang, T. X. Nie, J. M. Zhang, W. J. Jiang, Y. Wang, Y. G. Yao, L. He, and K. L. Wang, ACS Nano **7**, 9205 (2013).

[7]Bin Li, Qingyan Fan, Fuhao Ji, Zhen Liu, Hong Pan, and S Qiao, Phys. Lett. A **377**, 1925 (2013).

[8]Z. Zhang, X. Feng, M. Guo, K. Li, J. Zhang, Y. Ou, Y. Feng, L. Wang, X. Chen, K. He, X. Ma, Q. Xue, and Y. Wang, Nat. Commun. **5**, 4915 (2014).

[9]J. G. Checkelsky, R. Yoshimi, A. Tsukazaki, K. S. Takahashi, Y. Kozuka, J. Falson, M. Kawasaki, and Y. Tokura, Nat. Phys. **10**, 731 (2014).

[10]L. He, X. Kou, M. Lang, E. S. Choi, Y. Jiang, T. Nie, W. Jiang, Y. Fan, Y. Wang, F. Xiu, and K. L. Wang, Sci Rep **3**, 3406 (2013).